Supplementary Information

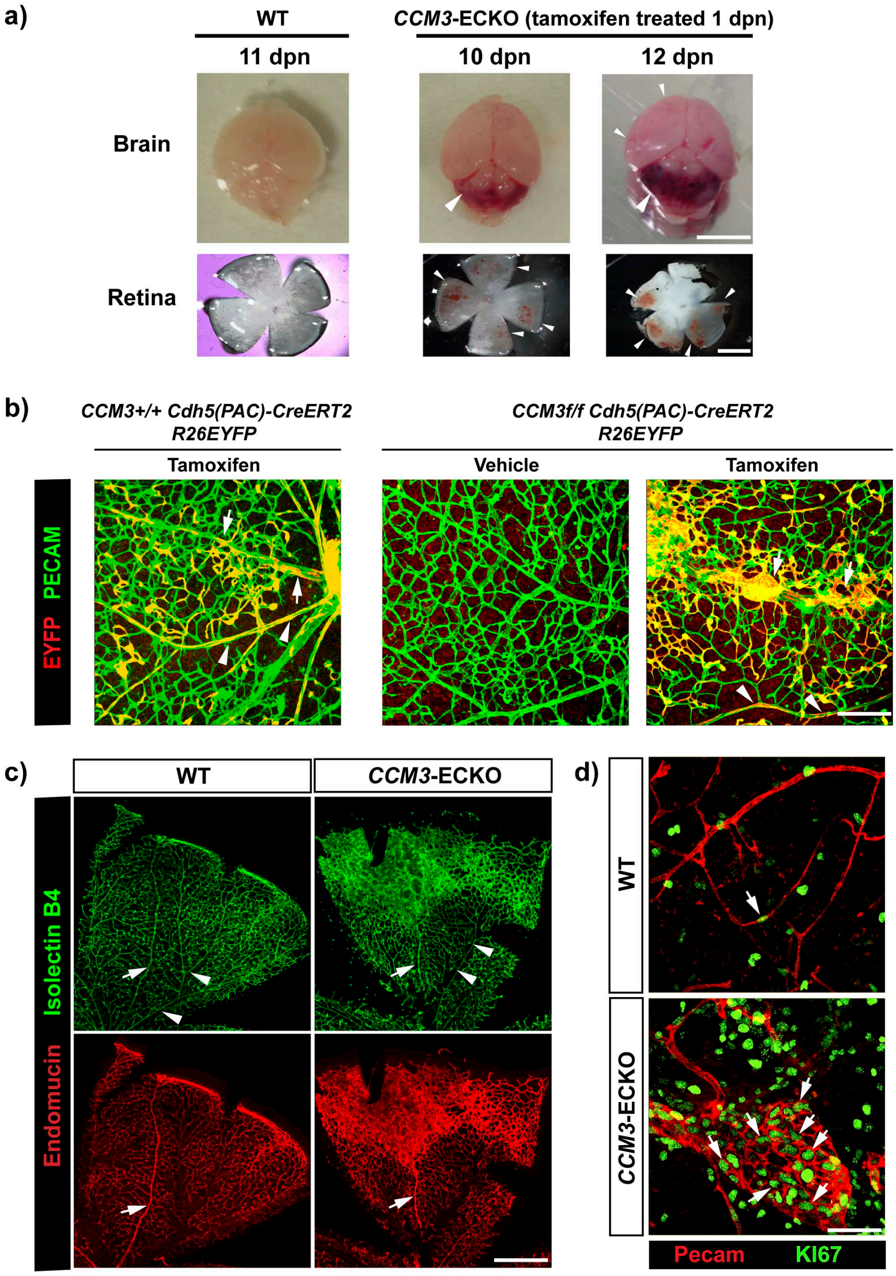

Figure S1. ***In vivo*** **model for endothelial-specific and inducible deletion of** ***CCM3*** **gene.** After endothelial-selective expression of Cre-recombinase in *CCM3*-flox/flox–*Cdh5(PAC)-CreERT2* mice (for tamoxifen-inducible endothelial-cell-specific expression of Cre-recombinase and *CCM3* gene recombination), the brain and retina of this mouse model show the formation of vascular lesions. These malformations develop from the venous vessels, even though Cre-recombinase is also active in the arteries. **a.** The *CCM3*-flox/flox–*Cdh5(PAC)-CreERT2* mice were treated with tamoxifen (10 mg/kg body weight, as described in Supplementary Information) at ^{1}dpn to induce endothelial-cell-selective expression of Cre-recombinase and recombination of the *CCM3*-flox/flox gene (*CCM3*-ECKO mice). The macroscopic appearance following dissection showed evident lesions in the cerebellum and retina (arrowheads). In the brain, some superficial vascular malformations can also be observed (small arrowheads), but most lesions can only be detected after sectioning and immunostaining, as shown in the main text. These lesions began to appear three to four days after treatment with tamoxifen, and they progressively increased in size. From 8 days after tamoxifen treatment, these *CCM3*-ECKO mice started to die, with evident hemorrhagic cerebellum. Tamoxifen did not induce any phenotype both in *CCM3*-flox/flox–*Cdh5(PAC)* mice negative for *CreERT2*, that did not express Cre-recombinase, and in the heterozygous *CCM3*-flox/$^{+}$–*Cdh5(PAC)-CreERT2* mice. The wild-type (WT) mice were *CCM3*$^{+/+}$–*Cdh5(PAC)-CreERT2* mice treated with tamoxifen. *CCM3*-flox/flox–*Cdh5(PAC)-CreERT2* mice treated with the Vehicle used to dissolve tamoxifen also showed a WT phenotype. Scale bar, 1cm. **b.** *CCM3*-flox/flox–*Cdh5(PAC)-CreERT2* mice were bred with *Rosa 26-Enhanced Yellow Green Fluorescent Protein* (*EYFP*) mice(1), kindly donated by Dr. S. Casola, IFOM, Milan, Italy, to monitor the expression of Cre-recombinase through the expression of EYFP. In vessels of the retina from *CCM3*$^{+/+}$–*Cdh5(PAC)-CreERT2–R26-EYFP* mice and *CCM3*-flox/flox–*Cdh5(PAC)-CreERT2–R26-EYFP* (*CCM3*-ECKO) mice, Cre-induced recombination (with tamoxifen treatment, as above) is indicated by the expression of the reporter gene EYFP. This was frequent in arteries (arrowheads), veins (arrows) and microvessels of both of these mouse models, and was seen as extensive co-localisation (yellow) of EYFP (red) and Pecam (green, marker of endothelial cells) labeling. The *CCM3* transcript was reduced by more than 80%, as assessed by RT-PCR in freshly isolated brain microvessels of *CCM3*-ECKO pups, in comparison to the tamoxifen-treated wild-type mice. Scale bar, 200 μm. **c.** In the retina of the *CCM3*-flox/flox–*Cdh5(PAC)-CreERT2* (*CCM3*-ECKO) mice, malformations only developed on the venous side of the vascular network, which can be distinguished morphologically in the retina (as in b.) and by endomucin-positive staining (red, arrows). Arrowheads indicate arterial vessels, which are endomucin negative and isolectin B4 positive (green). We have also observed a similar venous-specific defect after endothelial-specific ablation of both *CCM1(2)* and *CCM2(3)*. Scale bar, 700 μm. **d.** Magnification of brain vessels in WT and *CCM3*-ECKO mice. Endothelial cells (Pecam-positive, red) in the lesions present high number of KI67-positive nuclei (green) indicating active proliferation in comparison to WT. Scale bar, 30 μM. In (b) and (c) and (d) retinas from 9dpn matched littermate mouse pups are shown.

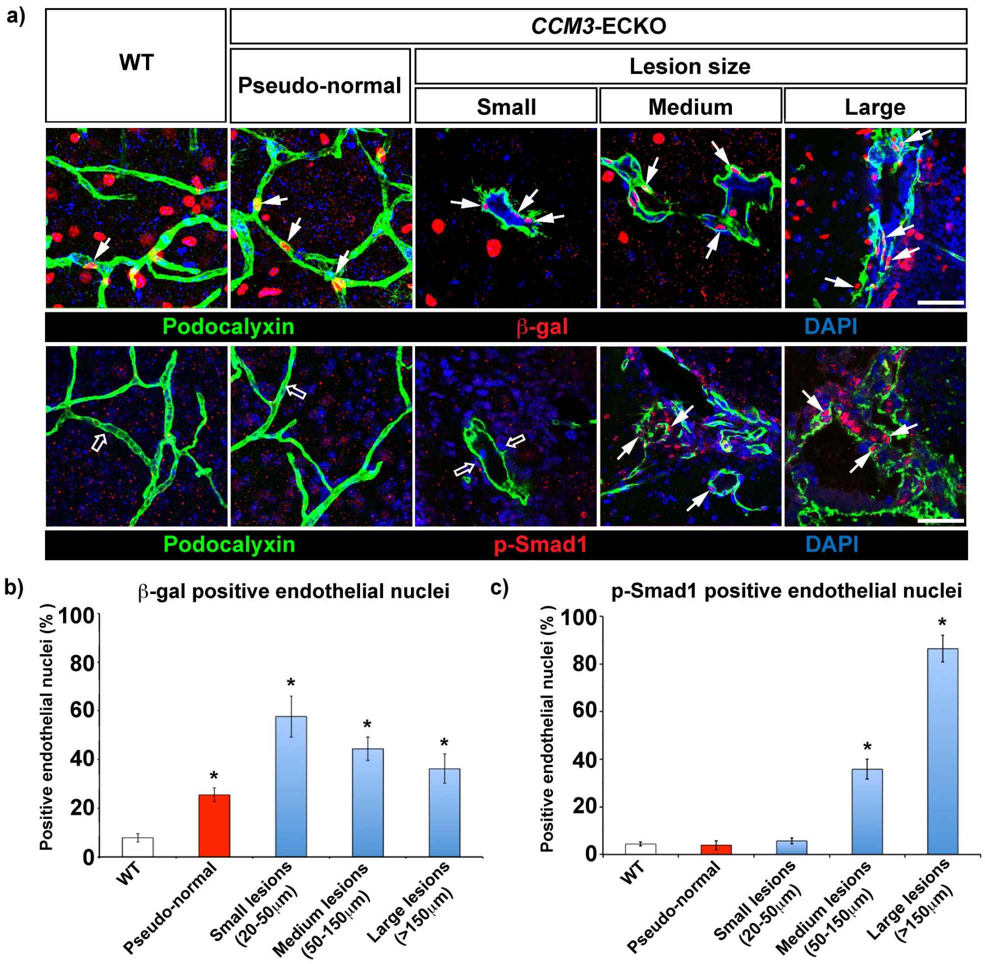

Figure S2. Brain endothelial cells in *CCM3*-ECKO mice show enhanced β-catenin-mediated transcription in lesions of any size as well as in pseudo-normal vessels while TGF-β/BMP signaling is detectable only in larger lesions.

a. Representative immunostaining for β-gal (red, upper panel) and p-Smad1 (phosphoSer463/465) (red, lower panel) in endothelial cells (Podocalyxin-positive, green) in brain sections from wild-type (WT) and *CCM3*-ECKO mice at 9dpn. Nuclei were stained with DAPI (blue). Pseudo-normal vessels as well as vascular lesions of increasing size are show in *CCM3*-ECKO. Arrows, p-Smad1- or β-gal-positive nuclei; empty arrows, p-Smad1-negative nuclei. Scale bar, 50 μm. Similar results were obtained using p-Smad3 antibody **b.** and **c.** Percentage of β-gal-positive or p-Smad1-positive endothelial nuclei on the total number of at least 250 endothelial nuclei counted for each condition. β−gal- and p-Smad1-positive and endothelial cell nuclei were counted in twenty random fields at 63× magnification in brain sections from matched littermate *CCM3*-ECKO (five) and WT (five) mice. *, p <0.05, t-test.

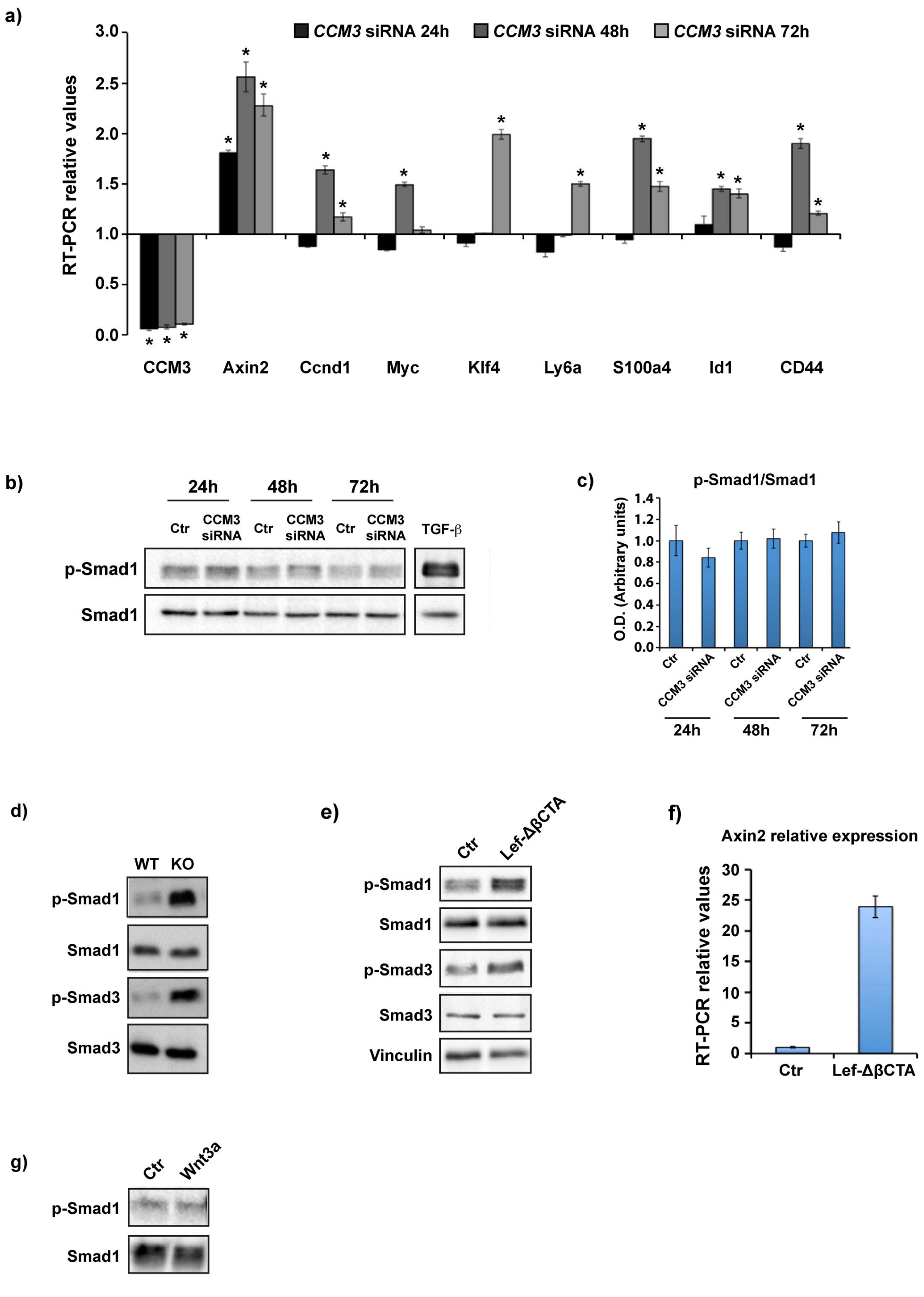

Figure S3. Acute down regulation of *CCM3* transcript activates transcription of β-catenin target genes and stem-cell/EndMT markers while it does not induce

Smad1 phosphorylation. Acute down regulation of *CCM3* transcript through siRNA (more than eighty percent inhibition by RT-PCR) in wild-type endothelial cells (cell line from not-recombined *CCM3*-flox/flox mice described in Fig.3b) induces transcription of typical β-catenin target genes (Axin2, Ccnd1, Myc) and EndMT markers (Klf4, Ly6a, S100a4, Id1, CD44), although with different kinetics. Axin2 is the earliest transcript to be enhanced (24 h), while the other ones show a delayed response (48-72 h). Transcripts were analyzed by RT-PCR at 24 h, 48 h, 72 h after a single *CCM3* siRNA transfection. Each time point has been compared with time-matched control. Controls were treated with negative (not-targeting) siRNA. Data are means (±SD) of three independent experiments. *, $p < 0.05$, t-test. **b**. Representative Western blot of p-Smad1 (phospho-Ser463/465) protein at different time points after *CCM3* siRNA. The same endothelial cell line shows phosphorylation of Smad1 after stimulation with TGF-β (0.5 ng/ml for 1 h) **c.** Ratio between p-Smad1 and total Smad1 normalized on respective Vinculin (housekeeper). Western blot bands have been quantified using ImageJ to calculate the ratios reported in the graph. Controls (Ctr) were treated with negative (not-targeting) siRNA. Data are means (±SD) of three independent experiments. **d.** Permanently *CCM3*-knockout endothelial cell line (KO) expresses increased level of both p-Smad1 and p-Smad3 under basal condition in comparison to wild-type (WT) as also reported after ablation of *CCM1*(2). **e.** Sustained activation of β-catenin-driven transcription (see in (**f.**) Axin2 RT-PCR level) by the constitutively active form of β-catenin Lef-ΔβCTA(4) induced phosphorylation of both Smad1 and Smad3. Lef-ΔβCTA was expressed for seven days after infection with Lentiviral construct(5). **g.** Acute stimulation with Wnt3a (for up to 24 h) could not stimulate Smad1 phosphorylation in Western blot.

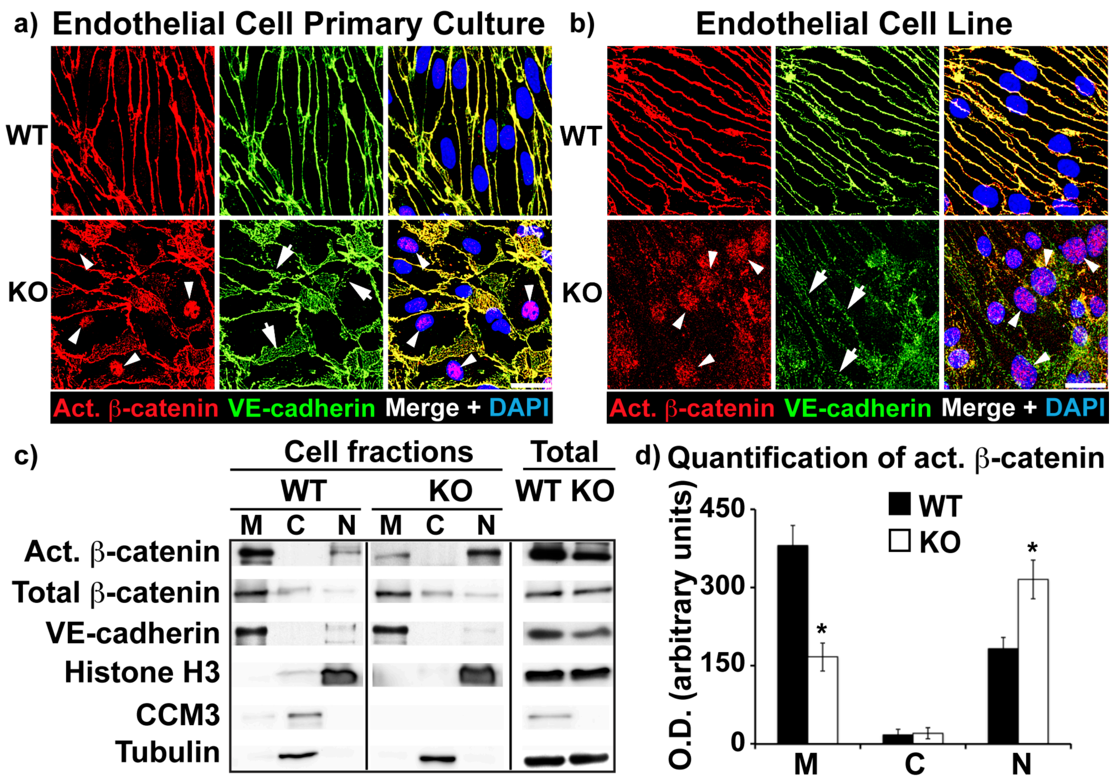

Figure S4. ***CCM3*****-knockout endothelial cells in culture show delocalization of active β-catenin from cell-cell junctions and its concentration into the nucleus.**

a, b. Brain (a) and lung (b) wild-type (WT) and *CCM3*-knockout (KO) endothelial cells stained for active (Act.) β-catenin (red) and VE-cadherin (green). Blue, DAPI-stained nuclei. Arrowheads, β-catenin-positive nuclei. Arrows, disorganized adherens junctions (VE-cadherin-staining). In *CCM3*-knockout endothelial cells, the *CCM3* transcript was reduced by 70%-90% (brain) and not detectable (lung) by RT-PCR, respectively. Scale bar, 20 μm. **c.** Cell fractionation and Western blotting of membrane (M), cytoplasm (C) and nucleus (N) compartments of lung wild-type (WT) and *CCM3*-knockout (KO) endothelial cells. Total active β-catenin was decreased by 34%-42%, and redistributed from membrane to nucleus as quantified in **d**. Mean (±SD) from three independent fractionations. *, $p < 0.05$ *versus* respective value in WT (t-test).

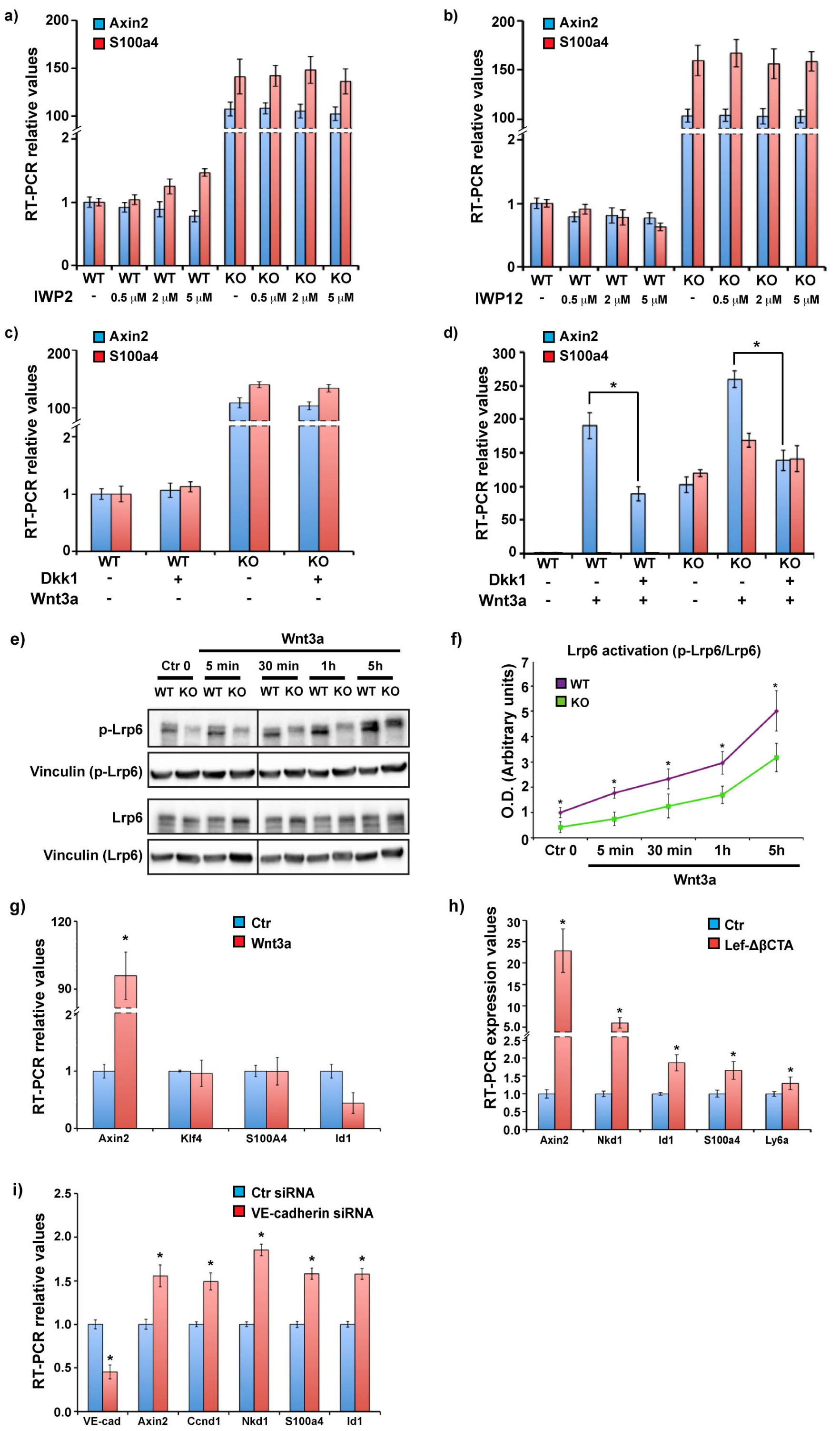

Figure S5. *CCM3*-knockout endothelial cells show cell-autonomous, Wnt-receptor independent activation of β-catenin signaling

a, b, c, d. β-catenin-driven activation of both Axin2 and S100a4 transcription in un-stimulated *CCM3*-knockout (KO) endothelial cells was not inhibited by either the porcupine inhibitors IWP2 or IWP12 (**a, b**) nor by the Lrp competitor Dkk1 (**c**) that effectively inhibited Wnt3a-induced stimulation of Axin2 both in wild-type and *CCM3*-knockout endothelial cell lines (**d**). Transcription of S100a4 was neither induced by Wnt3a in wild-type cells nor inhibited by Dkk1 in *CCM3*-knockout cells.

e, f. The Wnt co-receptor Lrp6 is less activated (phosphorylated) both in basal condition and after Wnt3a stimulation in *CCM3*-knockout in comparison to wild-type endothelial cells. Western blot representative of three independent experiments, quantified in (f), is shown. *, $p < 0.05$ *versus* WT (t-test). **g, h.** Acute stimulation (48 h) with Wnt3a cannot induce expression of stem-cell/EndMT markers in wild-type endothelial cells, while sustained stimulation (7 days), by-passing Wnt receptor, with constitutively active Lef-ΔβCTA does. *, $p < 0.05$ *versus* WT (t-test). **i.** Activation of typical β-catenin target genes (Axin2, Ccnd1, Nkd1) and stem-cell/EndMT markers (S100a4, Id1) is an early response to VE-cadherin silencing by siRNA (48 h) in wild-type endothelial cells. For analogous acute response to knockdown of CCM3 by siRNA see Supplementary Fig. S3. *, $p < 0.05$ *versus* negative control siRNA-treated cells (t-test).

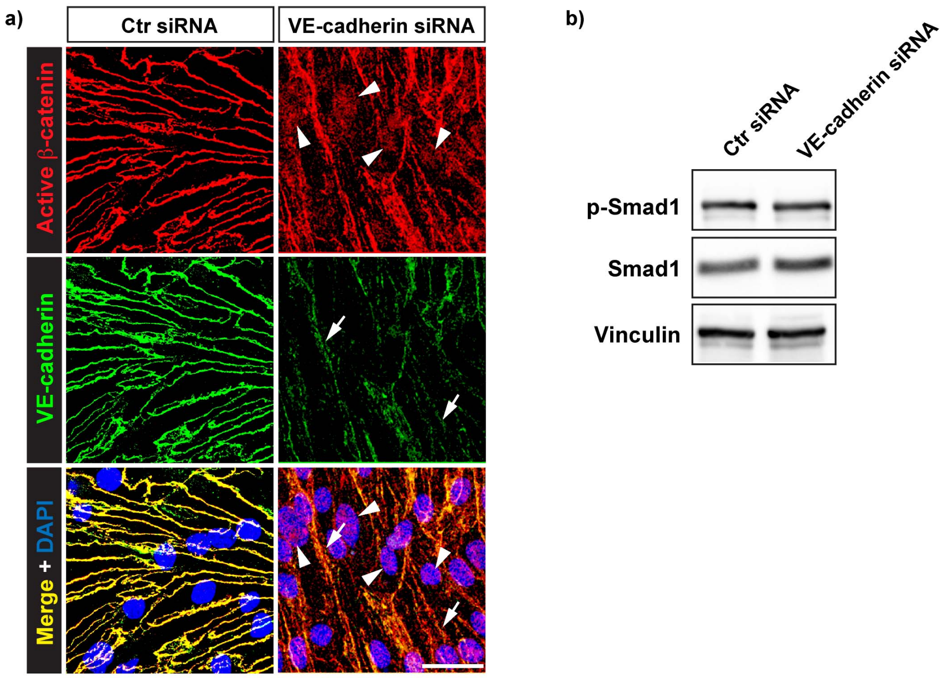

Figure S6. Junction dismantling following VE-cadherin silencing induces nuclear accumulation of active β-catenin in endothelial cells. However, Smad1 phosphorylation is not enhanced.

a. Representative immunostaining of active-β-catenin (red) and VE-cadherin (green) after VE-cadherin acute down regulation (48 h) through siRNA in wild-type endothelial cell line (described in Fig.3b). Junction dismantling and VE-cadherin down regulation (arrows) is accompanied by nuclear accumulation of active-β-catenin (arrowheads. DAPI indicating nuclei is in blue). Controls (Ctr siRNA) were treated with negative (not-targeting) siRNA. Scale bar, 30 μm. **b.** In the same cells VE-cadherin knockdown did not stimulate phosphorylation of Smad1 measured in Western blot.

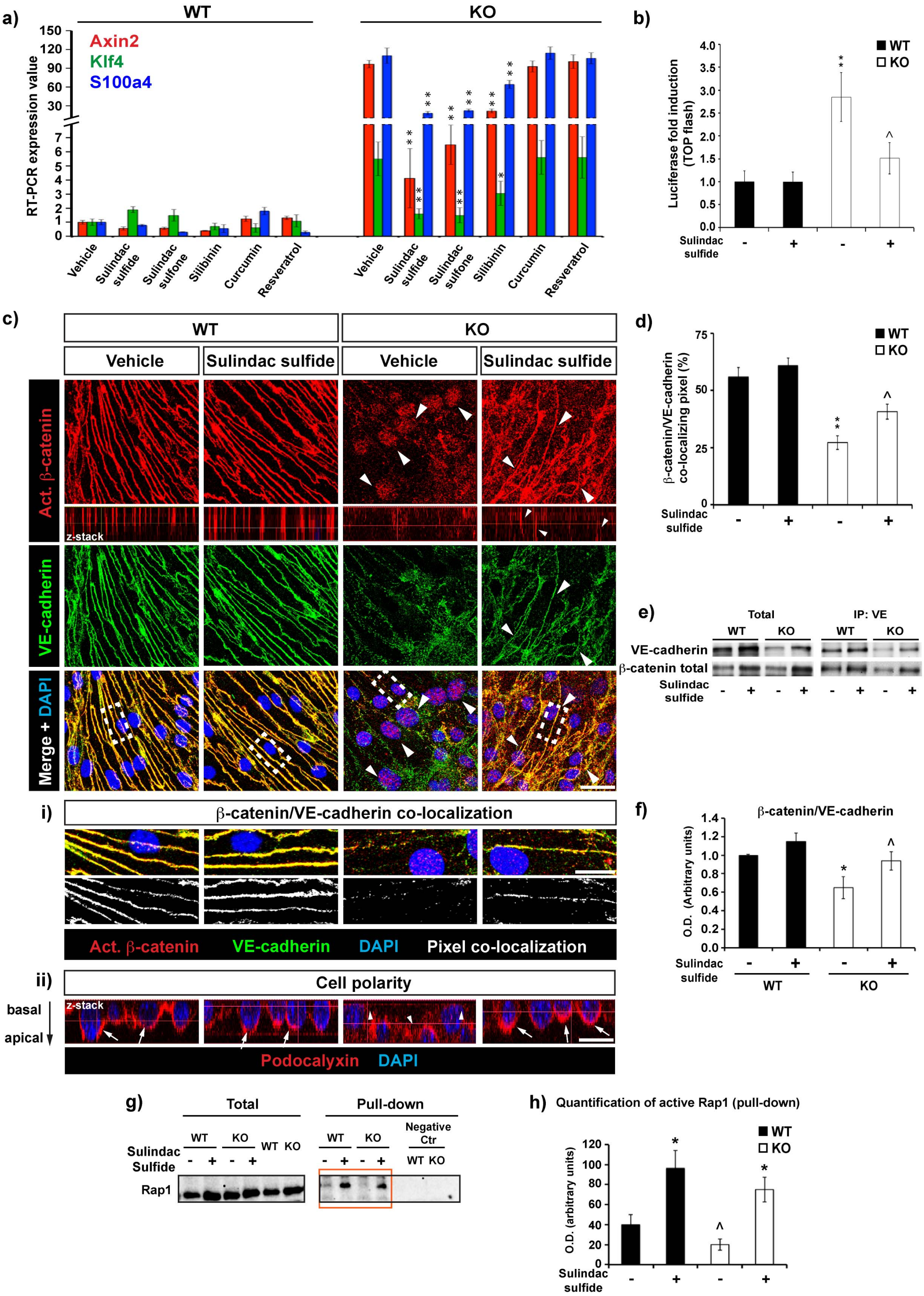

Figure S7. ***In vitro*** **screening of pharmacological antagonists of β-catenin signaling in** ***CCM3*****-knockout endothelial cells in culture and characterization of sulindac sulfide activity on** ***CCM3*****-knockout endothelial cells. a.** Quantification of effects of sulindac sulfide, sulindac sulfone, and other drugs that have been reported to target different steps of the β-catenin signaling pathway, on the overexpression of the β-catenin target gene, Axin2, and stem-cell/EndMT markers (Klf4, S100a4) in wild-type (WT) and *CCM3*-knockout (KO) endothelial cell line. Sulindac sulfide and sulindac sulfone show the greatest inhibition of the strong induction of transcription of Axin2, Klf4 and S100a4 seen in these *CCM3*-knockout endothelial cells. Among the other drugs tested here, silibinin was effective against these three transcripts. Data are mean RT-PCR values from at least three independent experiments, each carried out in triplicate. *, $p < 0.05$, **, $p < 0.01$ *versus* the respective transcripts in the Vehicle-treated *CCM3*-knockout endothelial cells (t-test). See Online Methods for further details. Comparable results were obtained with cells from between five and twenty-five passages after knockout of *CCM3*. **b.** Sulindac sulfide inhibited (^, $p < 0.05$, sulindac sulfide-KO *versus* Vehicle-KO, t-test) the significant increase (**, $p < 0.01$, Vehicle-KO *versus* Vehicle-WT, t-test) of β-catenin/Tcf4-dependent transcription of the luciferase reporter gene in the Top/Fop Flash assay (see Online Methods for details). The ratio between Top-flash and Fop-flash values normalized over transfection efficiency (β-galactosidase activity) is shown as fold change in comparison to the ratio in Vehicle-WT (relative Top/Fop-flash value). **c.** Representative immunostaining for effects of sulindac sulfide on re-localization of active β-catenin from the adherens junctions into the nucleus in wild-type (WT) and *CCM3*-knockout (KO) endothelial cell line. Active β-catenin (red) and VE-cadherin (green) were lost from cell-cell contacts (adherens junctions) in *CCM3*-knockout endothelial cells (top main panels, XY axis; small lower panels, Z projection along X axis). The active β-catenin is concentrated into the nucleus, as also seen in the merge with nuclei stained with DAPI (blue) (bottom panels, Vehicle, arrowheads). Co-localization of active β-catenin and VE-cadherin is shown in the Merge (yellow).

Treatment with sulindac sulfide restored the distribution of active β-catenin and VE-cadherin to the adherens junctions (right panels, sulindac sulfide, arrowheads, and small lower right panel, sulindac sulfide, small arrowheads, for distribution along Z axis). Scale bar, 30 μm. Bottom panels: **i.** β-catenin/VE-cadherin co-localization. Magnification of the boxed areas in Merge (yellow, upper panels) and segmentation of co-localization pixels (white, bottom panels), quantified in (**e**). Scale bar, 10 μm. **ii.** Cell polarity. Z projection along X axis: a marker of apical polarity in endothelial cells, Podocalyxin (red), shows loss of apical polarity in these *CCM3*-knockout endothelial cells. Podocalyxin is re-localized from the apical surface (left panels, WT, arrows) to be ectopically distributed on the basal side with *CCM3* knockout (Vehicle, arrowheads), as it has been reported for *CCM1* knockout(6). Sulindac sulfide re-establishes the correct apical distribution of Podocalyxin (right panel, sulindac sulfide, arrows). Scale bar, 15 μm. **d.** Quantification using Co-localization highlighter plugin of ImageJ software of the number of colocalizing pixels in conditions as in panel (c). Means (±SD) after quantification of fifteen different fields for each conditions from three independent experiments **, $p < 0.01$, Vehicle-KO *versus* Vehicle-WT; ^, $p < 0.05$, sulindac sulfide-KO *versus* Vehicle-KO, t-test. **e.** Representative Western blotting and quantification (f) of the effects of sulindac sulfide on the co-immunoprecipitation complex of β-catenin and VE-cadherin. Western blotting with the wild-type (WT) and *CCM3*-knockout endothelial cells of total extracts (Total) and immunoprecipitates with VE-cadherin antibodies (IP: VE). With sulindac sulfide treatment, the reduction in the level of VE-cadherin in the *CCM3*-knockout was restored (compare in Total: sulindac sulfide-KO and Vehicle-WT). **f.** With the co-immunoprecipitation complex measured as the β-catenin/VE-cadherin ratio, with sulindac sulfide treatment, the significantly reduced association between β-catenin and VE-cadherin in the *CCM3*-knockout (35% ±0.32 SD, *, $p < 0.05$, Vehicle-KO *versus* Vehicle-WT) was restored to the level observed in the wild-type cells (WT) (^, $p < 0.05$, sulindac sulfide-KO *versus* Vehicle-KO, t-test). Quantification of the bands from the Western blot was assessed as the means of three independent experiments, using ImageJ. **g.** Representative Western blot of Total and pulled-down (active) Rap1 in the indicated cell extracts. Although the total amount of Rap1 protein is slightly increased in *CCM3*-knockout endothelial cells, the amount of active Rap1 (GTP-bound, analysed through Rap1 pull-down assay, see Supplementary Methods) is down regulated in these cells. **h.** Quantification of Western blotting bands as in (g) using ImageJ (data are means (±SD) of three independent experiments). *, $p < 0.05$, sulindac sulfide *versus* Vehicle for both WT and *CCM3*-knockout, and ^, $p < 0.05$, *CCM3*-knockout *versus* WT (both Vehicle-treated), t-test. Negative control pull-down was with un-coupled Glutathione-Sepharose 4B beads.

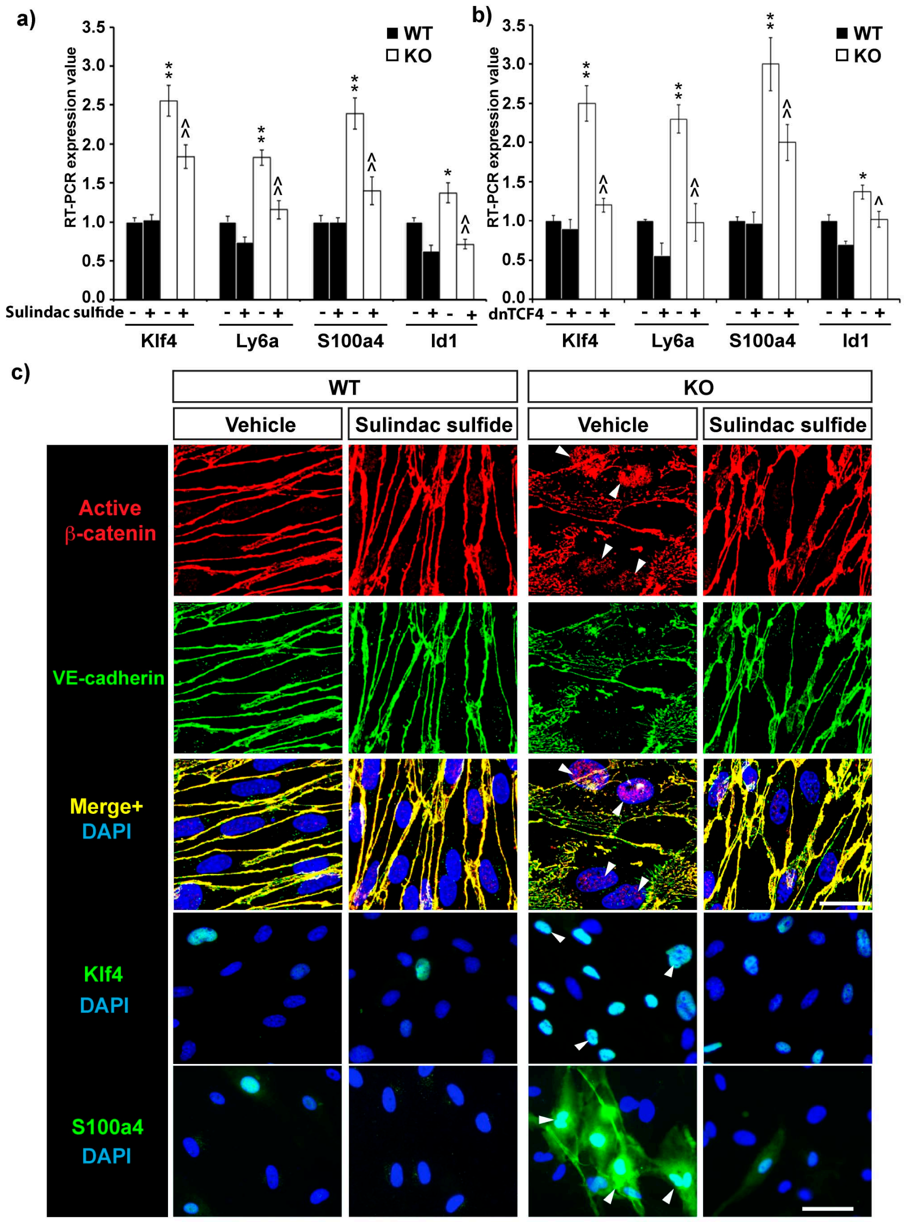

Figure S8. Brain *CCM3*-knockout endothelial cells show sulindac sulfide-inhibited transcription of β-catenin target genes and induction of re-localization of active β-catenin from the nucleus to adherens junctions.

a. Quantification of sulindac sulfide inhibition of expression of β-catenin target genes Klf4, Ly6a, S100a4 and Id1 (see b) by RT-PCR, in wild-type (WT) and *CCM3*-knockout endothelial cells in primary culture from brain (of *CCM3*-flox/flox mice and recombined *in vitro* as described in Fig. 3a). **, p <0.01(t-test) for the comparison *CCM3*-knockout *versus* WT under basal condition. ^, p <0.05; ^^, p <0.01 (t-test) for the comparison *CCM3* knockout plus sulindac sulfide *versus* Vehicle treated-*CCM3* knockout. **b.** dnTCF4 inhibits the overexpression of Klf4, Ly6a, S100a4 and Id1 in *CCM3*-knockout endothelial cells **c.** Representative immunostaining under sulindac sulfide treatment. Nuclei were stained with DAPI (blue). Top three rows: sulindac-sulfide-mediated redistribution of active β-catenin (red) from the nucleus (arrowheads) to cell-cell junctions in these *CCM3*-knockout endothelial cells. VE-cadherin (green) disorganization from junctions was also corrected by sulindac sulfide. Co-localization of active β-catenin and VE-cadherin is shown in the merge (yellow). Scale bar, 15 μm. Bottom two rows: sulindac sulfide inhibition of overexpression of Klf4 (green) and S100a4 (green) in these *CCM3*-knockout endothelial cells (turquoise shows co-localization with DAPI; arrowheads). Klf4 is exclusively nuclear and S100a4 is both nuclear and cytoplasmic in these *CCM3*-knockout brain endothelial cells. Scale bar, 30 μm.

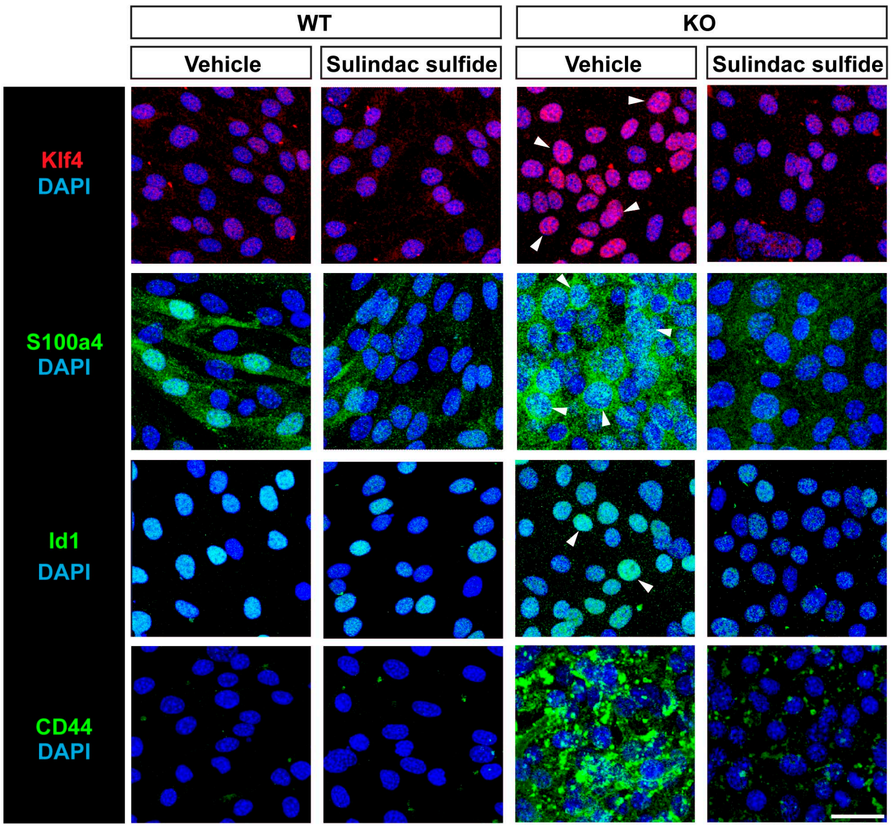

Figure S9. *CCM3*-knockout endothelial cells shows sulindac sulfide inhibition of overexpression of stem-cell/EndMT markers. Representative immunostaining showing that compared to the wild-type (WT), there was increased expression of Klf4, S100a4, Id1 and CD44 in *CCM3*-knockout (KO) endothelial cell line. Nuclei were stained with DAPI (blue). The overexpression of Klf4 (top row, red) and Id1 (third row, green) and with the *CCM3*-knockout was confined to the nucleus, as shown by double staining with DAPI (blue) (KO, Vehicle, arrowheads). Similarly, S100a4 (second row, green) was both nuclear and cytoplasmic (KO, Vehicle, arrowheads), while CD44 (bottom row, green) was mostly cytoplasmic (KO, Vehicle), Treatment with sulindac sulfide (right-hand panels) strongly reduced the overexpression of these proteins in *CCM3*-knockout (KO) endothelial cells. These results are comparable to the ones obtained in primary cultures of *CCM3*-knockout brain endothelial cells, as shown in Supplementary Figure S7. Scale bar, 30 μm.

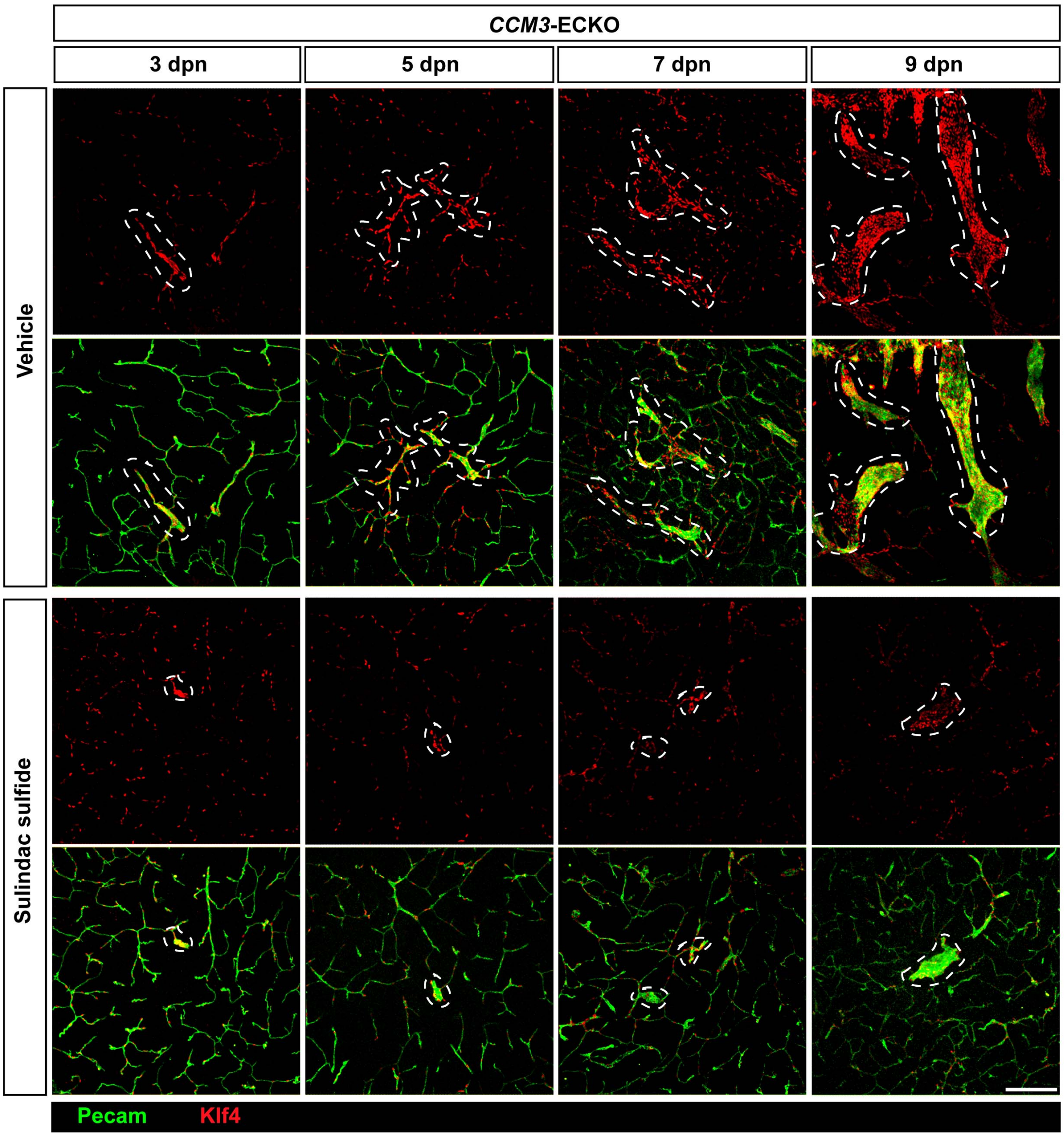

Figure S10. Sulindac sulfide reduces Klf4 overexpression in endothelial cells of brain vessels of *CCM3*-ECKO mice. Representative immunostaining for the effects of sulindac sulfide on Klf4 expression (red) in endothelial cells (Pecam-positive, green) of brain vessels of *CCM3*-ECKO mice at different time points after *CCM3* ablation at 1dpn. Sulindac sulfide treatment decreases the overexpression of Klf4 observed in endothelial cells of the vascular malformations in Vehicle-treated matched littermate pups. Klf4 is still expressed in the residual (although significantly contained, see Fig. 6) malformations that develop in sulindac sulfide-treated animals Dashed areas delineate CCM lesions. Scale bar, 700 μm.

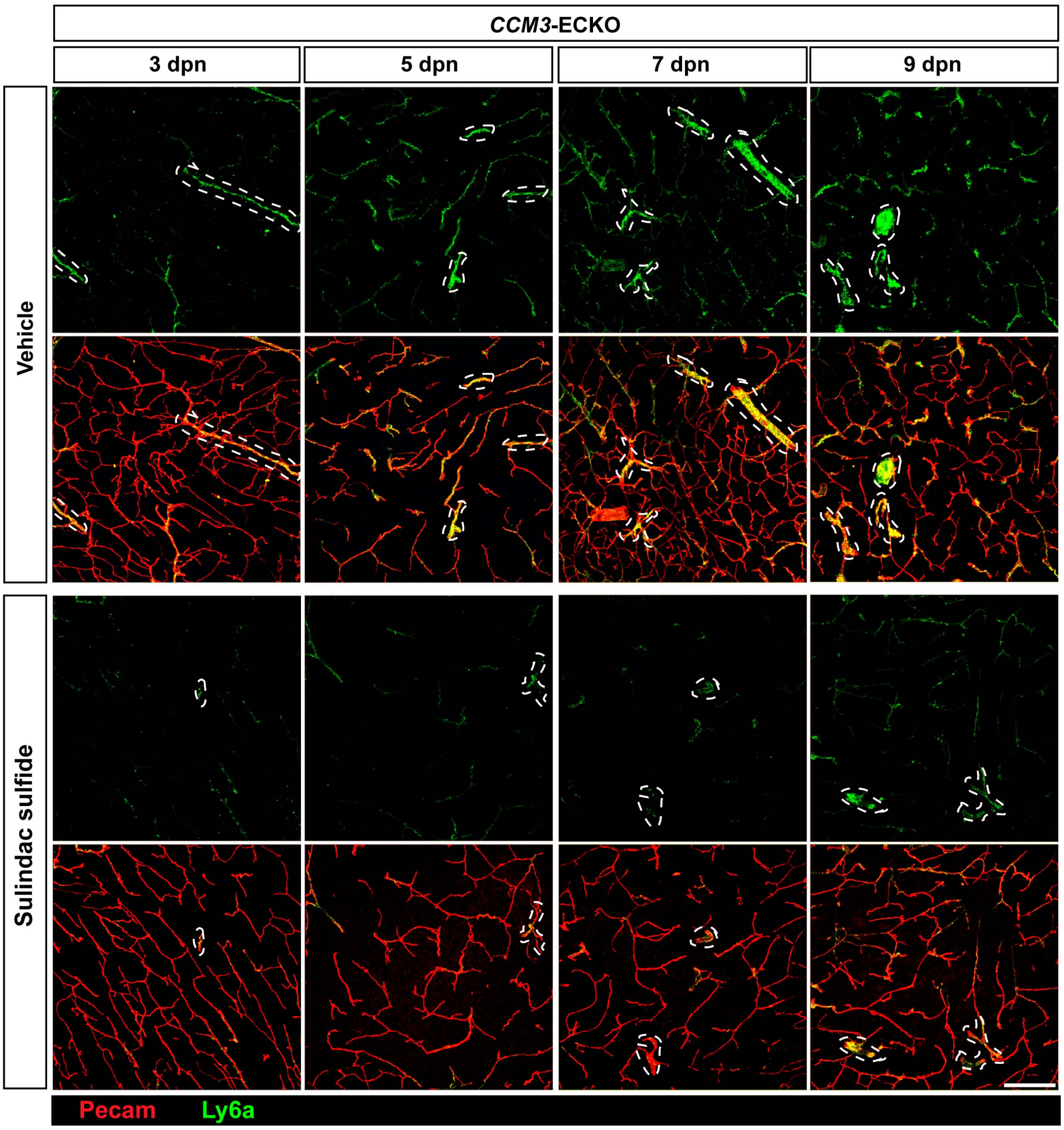

Figure S11. Sulindac sulfide decreases Ly6a overexpression in endothelial cells of brain vessels of *CCM3*-ECKO mice. Representative immunostaining for the effects of sulindac sulfide on Ly6a expression (green) in endothelial cells (Pecam-positive, red) of brain vessels of *CCM3*-ECKO mice at different time points after *CCM3* ablation at 1dpn. Sulindac sulfide treatment reduces the overexpression of Ly6a observed in endothelial cells of the vascular malformations in Vehicle-treated matched littermate pups. Ly6a is still expressed, although reduced, in the residual (although significantly restrained, see Fig. 6) malformations that develop in sulindac sulfide-treated animals. Dashed areas delineate CCM lesions. Scale bar, 700 μm.

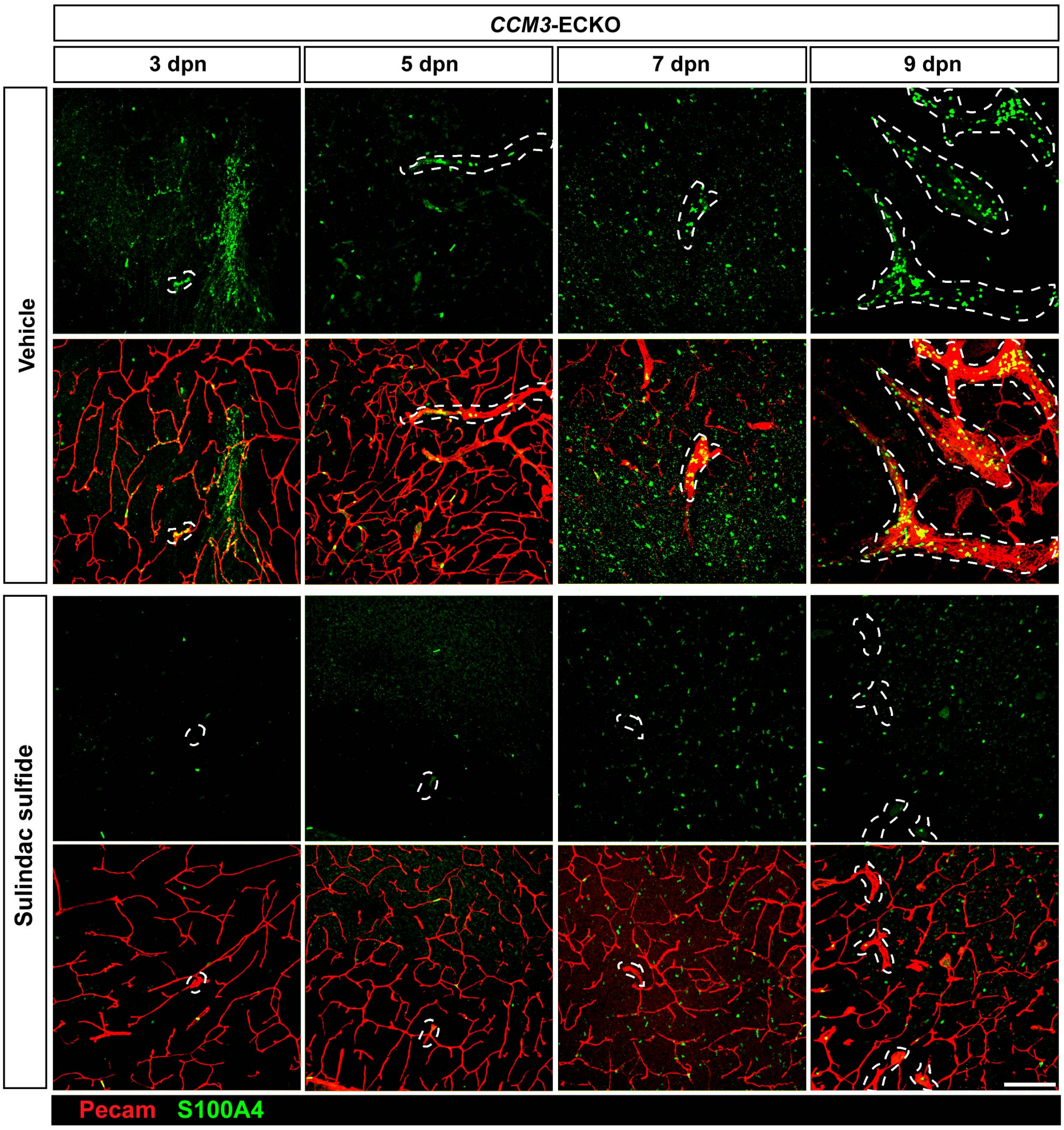

Figure S12. Sulindac sulfide decreases S100a4 overexpression in endothelial cells of brain vessels of *CCM3*-ECKO mice. Representative immunostaining for the effects of sulindac sulfide on S100a4 expression (green) in endothelial cells (Pecam-positive, red) of brain vessels of *CCM3*-ECKO mice at different time points after *CCM3* ablation at 1dpn. Sulindac sulfide treatment limits the overexpression of S100a4 observed in endothelial cells of the vascular malformations in Vehicle-treated matched littermate pups. S100a4 is strongly reduced also in the residual (although significantly reduced, see Fig. 6) malformations that develop in sulidac sulfide-treated animals. Dashed areas delineate CCM lesions. Scale bar, 700 μm.

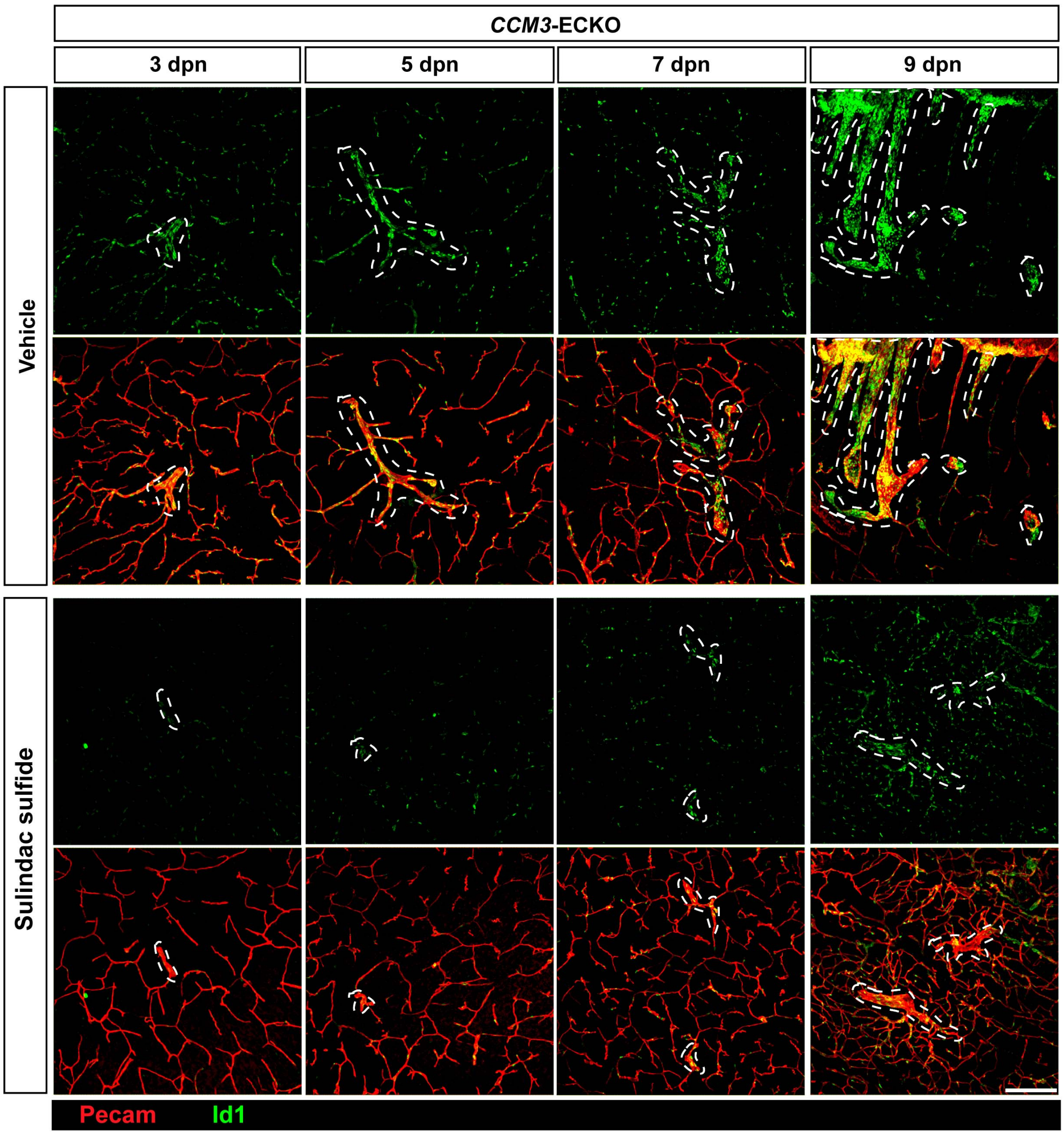

Figure S13. Sulindac sulfide reduces overexpression of Id1 in endothelial cells of brain vessels of *CCM3*-ECKO mice. Representative immunostaining for the effects of sulindac sulfide on Id1 expression (green) in endothelial cells (Pecam-positive, red) of *CCM3*-ECKO mice brain vessels at different ages after *CCM3* ablation at 1dpn. Sulindac sulfide treatment decreases the overexpression of Id1 observed in endothelial cells of the vascular malformations in Vehicle-treated matched littermate pups. Id1 is still expressed, although reduced, in the residual (although significantly decreased, see Fig.6) lesions that develop in sulidac sulfide-treated animals. Dashed areas delineate CCM lesions. Scale bar, 700 μm.

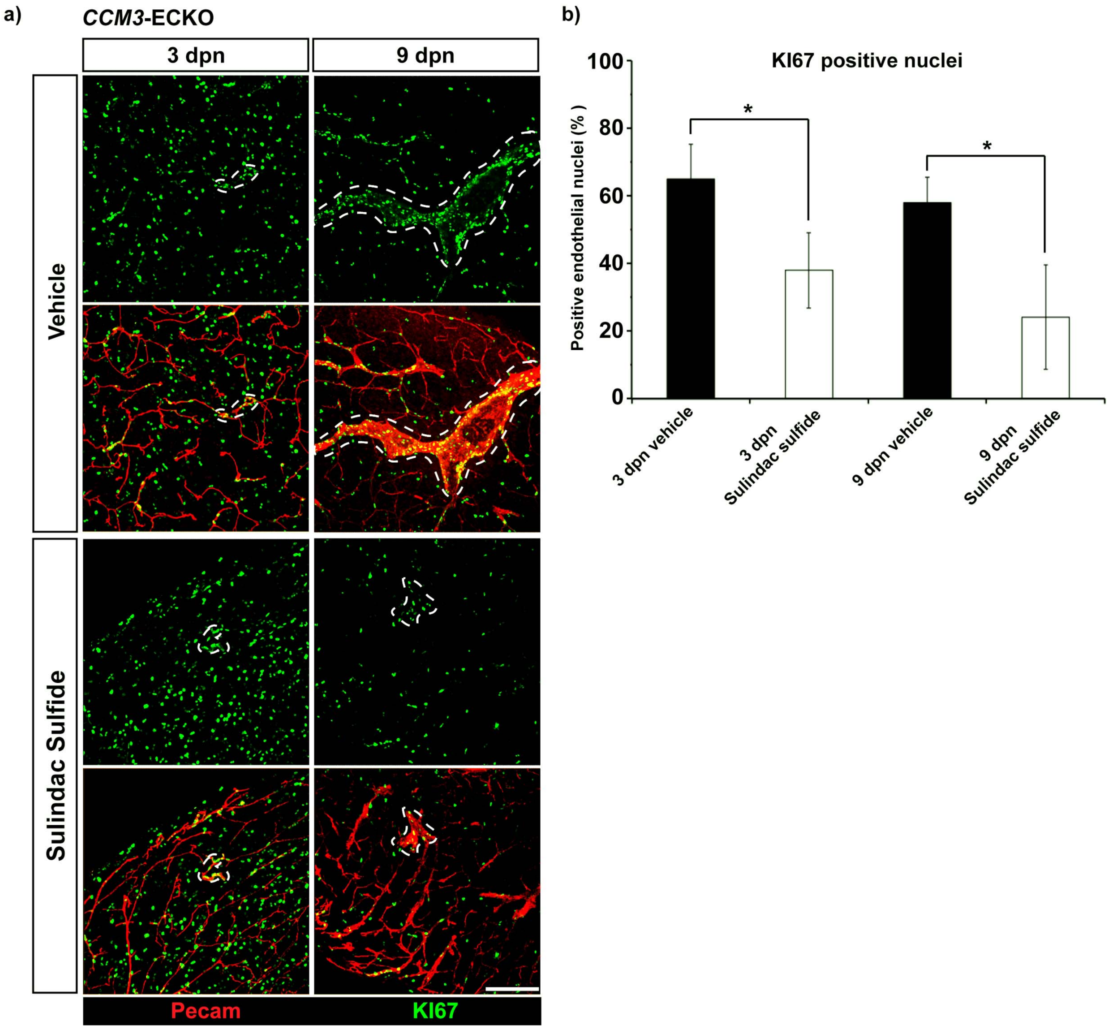

Figure S14. Sulindac sulfide limits endothelial cell proliferation in brain vessels of *CCM3*-ECKO mice. a. Representative immunostaining of the effect of sulindac sulfide on proliferation (KI67-positive nuclei, green) of endothelial cells (Pecam-positive, red) in brain vessels of *CCM3*-ECKO mice at different time points after *CCM3* ablation at 1dpn. Dashed areas delineate CCM lesions. **b**. Quantification as percentage of KI67-positive nuclei in endothelial cell in brain lesions of *CCM3*-

ECKO mice at 3 and 9dpn. Endothelial cell nuclei were counted in twenty random fields at 63× magnification in brain sections from five *CCM3*-ECKO mice and five matched littermate WT mice at each time points. A total number of at least 250 nuclei were counted for each condition. The comparison between Vehicle- and sulindac sulfide-treatment is shown. Scale bar, 700 μm. *, $p < 0.05$ sulindac sulfide treatment *versus* Vehicle at each time point (t-test).

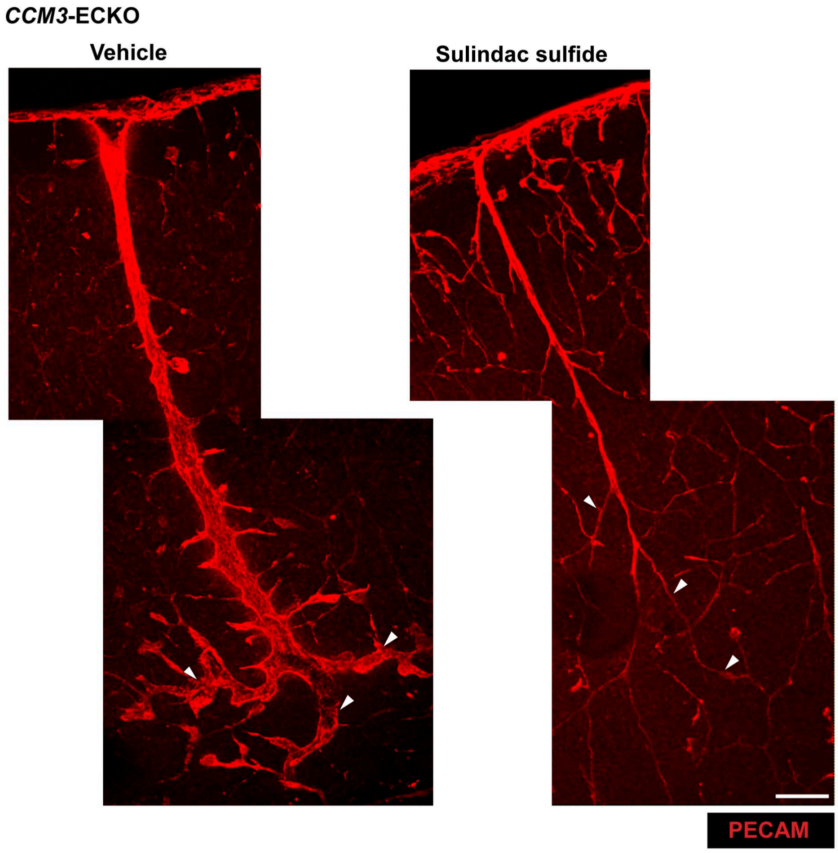

Figure S15. Sulindac sulfide reduces the diameter of abnormally enlarged brain vessels in *CCM3*-ECKO mice. *CCM3*-ECKO pups (at 9dpn, with *CCM3* recombination at 1dpn) treated (from 2dpn) with Vehicle or sulindac sulfide (littermate pups), as described in the Online Methods, show sulindac sulfide reduction of the malformations in cerebral vessels. Representative immunostaining of brain sections with Pecam (red, endothelial cells) of vessels of the superior sagittal sinus that enter the brain from the dorsal surface. With the *CCM3*-ECKO (Vehicle), the straight vessels with large diameters are seen to terminate in budding branches that form cavernae (arrowheads). In a comparable vessel of a matched *CCM3*-ECKO littermate pup, sulindac sulfide treatment greatly reduces the diameter and promotes apparently normal terminal branching (arrowheads). The panels show maximal projections of confocal optical sections of samples acquired at 20× magnification. Scale bar, 100 μm. Scale bar, 100 μm.

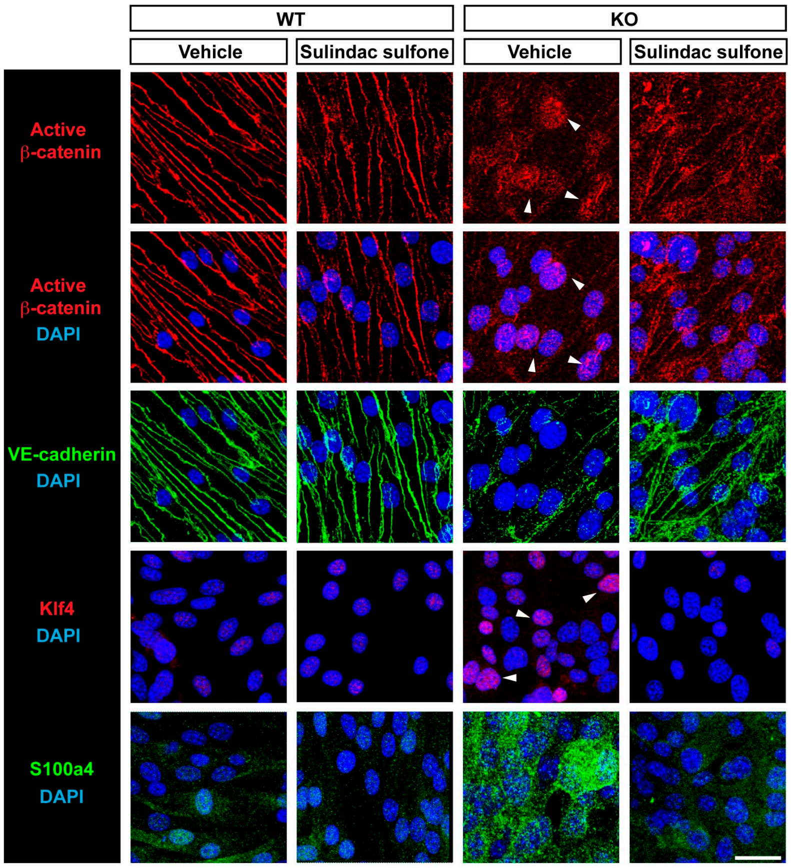

Figure S16. Sulindac sulfone inhibits the expression of β-catenin-driven stem-cell/EndMT markers and induces the re-localization of active β-catenin from the nucleus to adherens junctions in *CCM3* null endothelial cells in culture. Similar to the effects of sulindac sulfide, *CCM3*-knockout endothelial cell line show sulindac sulfone inhibition of loss of active β-catenin and VE-cadherin from cell-cell contacts (adherens junctions), of accumulation of active β-catenin in the nucleus, and of overexpression of stem-cell/EndMT markers. Representative immunostaining showing that the loss of active β-catenin (red) from cell-cell contacts (top row) and its re-localization to the nucleus (second row) in these *CCM3*-knockout endothelial cells (KO, Vehicle, arrowheads) was inhibited by sulindac sulfone treatment. Nuclei were stained with DAPI (blue). Similarly, VE-cadherin (green) loss from cell-cell contacts was inhibited by sulindac sulfone treatment (third row). Overexpression of Klf4 (red; nuclear, Vehicle, arrowheads) and S100a4 (green; cytoplasmic and nuclear) in these *CCM3*-knockout (KO) endothelial cells was also strongly reduced by sulindac sulfone treatment (bottom rows). Scale bar, 30 μm.

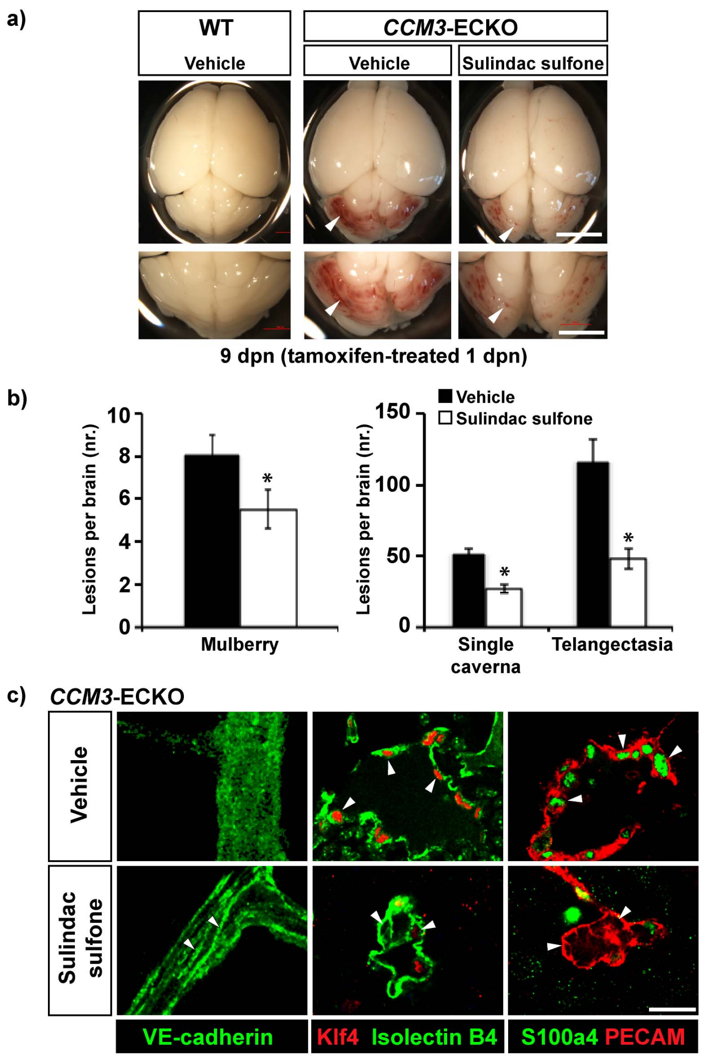

Figure S17. Sulindac sulfone reduces the vascular lesions in the brain and retina vessels of *CCM3*-ECKO mice. Similar to the effects of sulindac sulfide *CCM3*-flox/flox–*Cdh5(PAC)-CreERT2–BAT-gal* (*CCM3*-ECKO) mice show sulindac sulfone reduction of the malformations in cerebral vessels. These mice were treated with tamoxifen (10 mg/kg body weight, as described in Online Methods) at 1dpn to induce endothelial-cell-selective expression of Cre-recombinase and recombination of the flox/flox *CCM3* gene (*CCM3*-ECKO mice). They were also treated with Vehicle or with sulindac sulfone (30 mg/kg) daily, starting from 2dpn. **a.** The macroscopic appearance of the 9dpn mouse pup brains following dissection showed evident lesions in the cerebellum of the *CCM3*-ECKO mice (arrowheads), which were reduced by sulindac sulfone (arrowheads). Scale bar, 0.65 cm. Lower panels: Further magnification of the cerebellum. Scale bar, 0.3 cm. **b.** Quantification of mean brain lesions as the mulberry (multiple lumens), single caverna, or telangiectases lesions in the entire brains (as described in(7), see Online Methods) from five Vehicle-treated and five sulindac-sulfone-treated *CCM3*-knockout matched littermate pups. The brains were sectioned along the sagittal axis (150 μm sections, vibratome), immunostained for Pecam (endothelial cells) and examined by wide-field fluorescence microscopy (10× and 20× magnification). *, $p = 0.0053, 0.006, 0.004$ for mulberry, single caverna and telangiectase lesions, respectively (Wilcoxon test). **c.** Representative immunostaining of localization of VE-cadherin, Klf4 and S100a4. Left: From the diffuse state of VE-cadherin (green) in Vehicle-treated *CCM3*-ECKO mice, sulindac sulfone restored its localization to cell-cell junctions (arrowheads). Middle, right: From the nuclear staining for the expression of Klf4 (middle, red; green, isolectinB4, endothelial cells) and S100a4 (right, green; red, Pecam, endothelial cells) in endothelial cells of Vehicle-treated *CCM3*-ECKO mice (arrowheads), sulindac sulfone reduced this nuclear reactivity for both Klf4 and S100a4 (arrowheads). Scale bar, 15 μm.

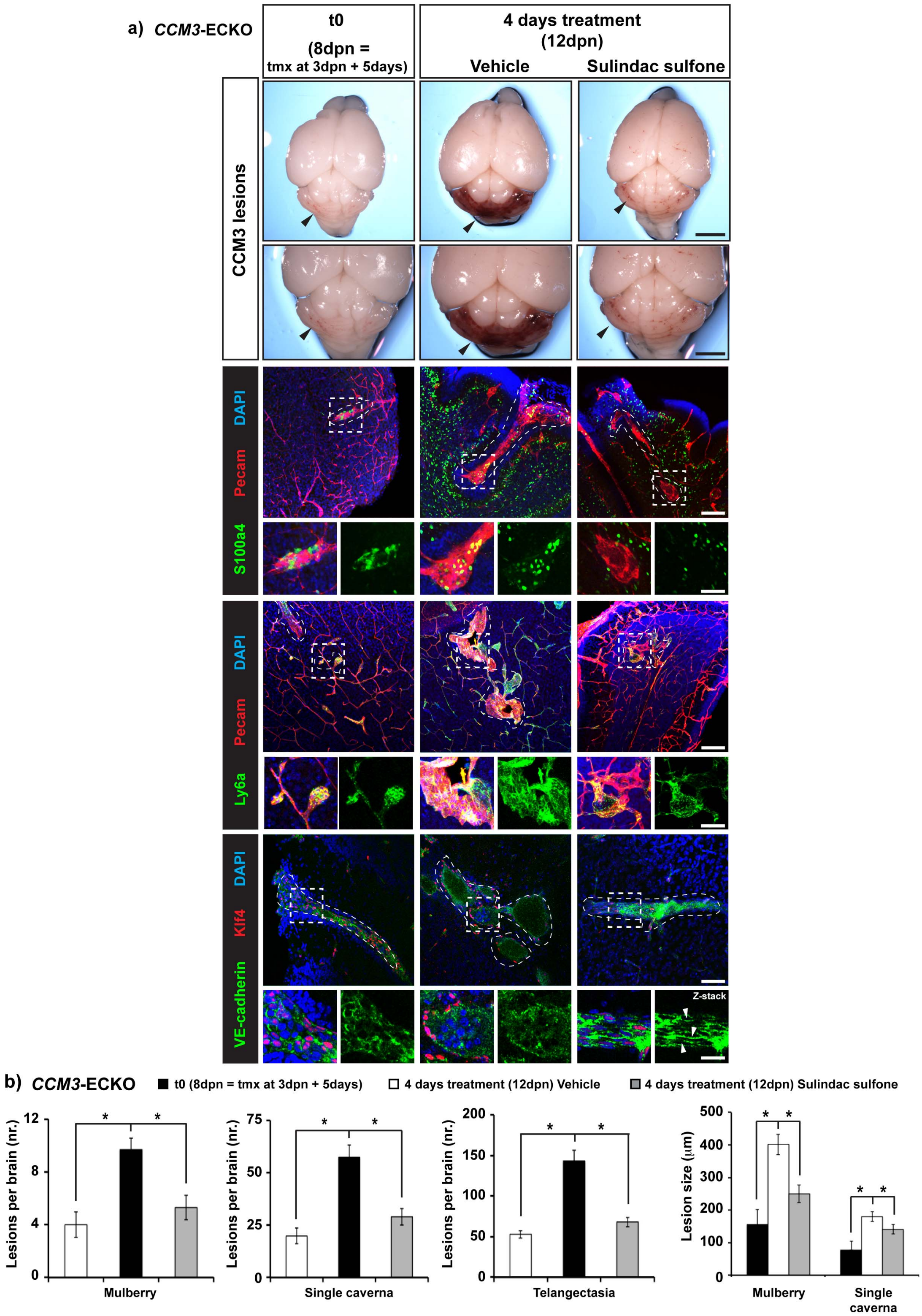

Figure S18. Sulindac sulfone limits the progression of established CCM lesions in *CCM3*-ECKO mice. *CCM3*-flox/flox–*Cdh5(PAC)-CreERT2–BAT-gal* mice were treated with tamoxifen (tmx, 10 mg/kg body weight, as described in Online Methods) at 3dpn to induce endothelial-cell-selective expression of Cre-recombinase and recombination of the flox/flox *CCM3* gene (*CCM3*-ECKO mice). Delayed recombination was used to induce a milder phenotype and extend the life span of recombined animals (3). Mice were also treated with Vehicle or with sulindac sulfone (30 mg/kg) daily, starting from 8dpn, that is allowing five days for CCM lesions to establish as shown in the left column panels in (a). **a.** Six upper panels: macroscopic appearance of (t0), the 8dpn mouse pup brain on the day of beginning of sulindac sulfone administration and of (4 days treatment), the 12dpn mouse pup brains after four days treatment with Vehicle or sulindac sulfone. Evident lesions in the cerebellum, already present at t0 (arrowheads), were constrained by sulindac sulfone in comparison to Vehicle. Scale bar, 0.65 cm. Magnification: scale bar, 0.3 cm. Lower panels: representative immunostaining of the EndMT markers S100a4, Ly6a and Klf4 (small panels, magnification of the boxed areas for S100a4/Pecam and Ly6a/Pecam, magnification and Z-stack for Klf4/VE-cadherin staining). Sulindac sulfone limits the nuclear staining for S100a4 (top, green; red, Pecam-positive endothelial cells) and Klf4 (bottom, red; green, VE-cadherin-positive endothelial cells) in endothelial cells of Vehicle-treated *CCM3*-ECKO mice Also Ly6a immunostaining (middle, green: red, PECAM-positive endothelial cells), was contained by sulindac sulfone. Immuno-reactivity for these EndMT markers was already present at t0. From the diffuse state of VE-cadherin (green) in Vehicle-treated *CCM3*-ECKO mice, sulindac sulfone restored its localization to cell-cell junctions (Z-stack, arrowheads). Nuclei were stained with DAPI (blue). Scale bar, 700 μm. Magnification: scale bar, 20 μm. **b.** Left and middle panels: quantification of mean number of brain lesions as illustrated in (a). Matched littermates from three independent litters were sacrificed at t0 (n=4) or Vehicle-treated (n=4) or sulindac sulfone-treated (n=4). *, $p < 0.005$, Wilcoxon signed-rank test. Right-hand panel: quantification of mean size of brain lesions (μm, see Online Methods for details). *, $p < 0.05$, t-test.

Supplementary methods

Endothelial-cell-specific recombination in CCM3-flox/flox mice

These *CCM3*-flox/flox mice were bred with *Cdh5(PAC)-CreERT2* mice(8) (kindly donated by Dr. R.H. Adams, University of Munster, Muenster, Germany), for tamoxifen-inducible endothelial-cell-specific expression of Cre-recombinase and *CCM3* gene recombination. The *CCM3*-flox/flox–*Cdh5(PAC)-CreERT2* mice were further bred with *BAT-gal* mice(9) (kindly donated by Dr. S. Piccolo, Padova, Italy), to monitor the activation of β-catenin transcription signaling, and with *Rosa 26-Enhanced Yellow Green Fluorescent Protein (EYFP)* mice(1) (kindly donated by Dr. S. Casola, IFOM, Milan, Italy), to monitor the expression of Cre-recombinase through the expression of EYFP. Tamoxifen (Sigma) was dissolved in corn oil and 10% ethanol (at 10 mg/ml), and then diluted 1:5 in corn oil before single intragastric administration to 1-2dpn pups (35 mg/kg body weight), as described in(8). The control (wild-type) mice included *CCM3*-flox/flox–*Cdh5(PAC)-CreERT2–BAT-gal* mice treated with the Vehicle used to dissolve the tamoxifen (corn oil plus 2% ethanol), and *CCM3*$^{+/+}$*–Cdh5(PAC)-CreERT2–BAT-gal* mice treated with tamoxifen. The mouse genotyping through genomic PCR is described in the following section.

Mouse genotyping

The following probes were used for the mouse genotyping: wild-type *CCM3* allele: 5’ GAT AGG AAT TAT TAC TGC CCT TCC 3’, 5’ GAC AAG AAA GCA CTG TTG

ACC 3’; deleted *CCM3* gene after recombination induced by Cre-recombinase: 5’ GAT AGG AAT TAT TAC TGC CCT TCC 3’, 5’ GCT ACC AAT CAG CTT CTT AGC CC 3’, *Cdh5(PAC)-CreERT2* gene: 5' CCA AAA TTT GCC TGC ATT ACC GGT CGA TGC 3', 5' ATC CAG GTT ACG GAT ATA GT 3'; *BAT-gal* gene: 5' CGG TGA TGG TGC TGC GTT GGA 3', 5' ACC ACC GCA CGA TAG AGA TTC 3'; *Rosa 26 EYFP* gene: 5' GCG AAG AGT TTG TCC TCA ACC 3', 5' GGA GCG GGA GAA ATG GAT ATG 3, 5' AAA GTC GCT CTG AGT TGT TAT 3'

RT-PCR

RNA extraction was performed with RNeasy kits (74106; Promega). The RNA (1 μg) was reverse transcribed with random hexamers (High Capacity cDNA Archive kits; Applied Biosystems). The cDNA was amplified with TaqMan gene expression assays (Applied Biosystems) using a 7900 HT thermocycler (ABI/Prism). For each sample, the expression levels were determined with the comparative threshold cycle (Ct) method, and normalized to the housekeeping genes encoding 18S and glyceraldehyde-3-phosphate dehydrogenase (GAPDH). For amplification, validated probes were used (Applied Biosystem; see Supplementary Online Methods). The probes to identify the *CCM3* mRNA transcript were custom designed, as: forward, CGAGTCCCTCCTTCGTATGG; reverse, GCTCTGGCCGCTCAATCA; reporter sequence, CTGATGACGTAGAAGAGTACA.

Probes (Applied Biosystems) that have been validated to recognize the following mouse transcripts in RT-PCR were used: Axin2, Lef1, Ccnd1, Klf4, Ly6a, S100a4, Id1, CD44, Nkd1, VE-cadherin, Cdh2, Bmp2, Bmp6, Acta2.

Antibodies

The following antibodies were used: anti-Pecam (hamster; MAB1398Z, Millipore); anti-β-galactosidase (chicken; ab9361, Abcam); anti-VE-cadherin (rat monoclonal; 550548, BD Biosciences); anti-VE-cadherin (goat; sc-6458, Santa Cruz); anti-active-β-catenin (mouse monoclonal; clone 8E7, dephosphorylated on Ser37 and Thr41, Millipore); anti-total-β-catenin (mouse monoclonal, Cell Signaling); anti-S100a4 (rabbit; 07-2274, Millipore; anti-p-Smad1 (Ser463/465) (rabbit, BA3848, Millipore), anti-p-Smad1 (rabbit; 9516, Cell Signaling); anti-Smad1 (rabbit; 6944, Cell Signaling); anti-p-Smad3 (rabbit; 18801, Epitomics); anti-Smad3 (rabbit; 9523, Cell Signaling); anti-p-Lrp6 (Ser1490) (rabbit; 2568, Cell Signaling); anti-total Lrp6 (rabbit; 3395, Cell Signaling); anti-Vinculin (mouse; V9131, Sigma); anti-Rap1 (rabbit; Sc-65, Santa Cruz); anti-Histone H3 (rabbit; ab1791, Abcam); anti-Klf4 (goat; AF3158, R&D); anti-CD44 (rat; 553131, BD Biosciences); anti-Id1 (rabbit; sc-488, Santa Cruz); anti-αSMA (mouse monoclonal; F3777, Sigma); anti-GFP (rabbit; A-6455, Invitrogen); anti-Podocalyxin (goat; AF1556, R&D); anti-p-Histone H3 (rabbit; ab51776, Millipore); anti-KI67 (rabbit; Ab1667, Abcam); anti-CCM3 (rabbit; Eurogentec); anti-α-tubulin (mouse monoclonal; T9026, Sigma). Biotin-conjugated isolectin B4 (Vector Lab), revealed with Alexa555-conjugated streptavidin (Molecular Probes), was also used to identify endothelial cells in retina and brain sections. The secondary antibodies for immunofluorescence were anti-Alexa448 and anti-Alexa555, and Cy3-conjugated antibodies raised in the donkey against the immunoglobulin of the appropriate animal species (Molecular Probes or Jackson Laboratories). The secondary antibodies for Western blotting were HRP-linked anti-mouse, anti-rat and anti-rabbit antibodies (Cell Signaling), and HRP-linked anti-goat antibodies (Promega).

In-vitro isolation, culture and recombination of endothelial cells from the CCM3-flox/flox mice

Recombination of the floxed *CCM3* gene was induced by treating the cells at culture day 1 with the AdenoCre viral vector (*CCM3*-knockout endothelial cells), as previously described(10). The control endothelial cells (wild-type) were an aliquot of the same endothelial cell preparation treated with AdenoGFP, instead of AdenoCre. The cells were then maintained in culture for up to a further 7 days before analysis, as described in the main text. Drug treatments were for 48 h before the processing of the cells as described in Supplementary Information.

In some experiments, endothelial cell lines from the lungs of *CCM3*-flox/flox mice (8-10 weeks old) were immortalized in culture through retroviral expression of polyoma middle T gene(11). Ablation of the *CCM3* gene was achieved with the AdenoCre viral vector (with AdenoGFP in the control cells, wild-type endothelial cell line). After deletion of *CCM3* (*CCM3*-knockout endothelial cell line), the cells were maintained in culture for up to 25 passages without detectable changes in the effects of this *CCM3* ablation. These endothelial cell lines responded to the absence of CCM3 in a comparable way to both primary cultures of brain endothelial cells *in-vitro* and brain endothelial cells *in-vivo*.

Drug treatment of cells in culture

Drugs were added to confluent cells for 48 h before the indicated assays. Final concentrations used were: 135 μM sulindac sulfide, 125 μM sulindac sulfone, 200 μM silibinin, 40 μM curcumin, 40 μM resveratrol, 0.5, 2, 5 μM IWP2 and IWP12 (all from Sigma-Aldrich). As all drugs were dissolved in DMSO, control treatment

(Vehicle) was 0.1% DMSO final concentration, as for drug treatment. Murine recombinant Dkk1 (0.5 μM on cells) was from R&D.

siRNA

CCM3 and VE-cadherin expression were silenced using siRNA oligos to murine CCM3 (Stealth RNAi, Invitrogen) and to murine VE-cadherin (Smart pool, Thermo Scientific), respectively, and Lipofectamine 2000 for transduction as described in(6).

Immunofluorescence microscopy of brain sections, retinas and cells in culture

Brains and eyes from mice pups were fixed in 3% paraformaldehyde immediately after dissection, and this fixing was continued overnight at 4 °C. The retinas were dissected from the eyes just before staining as the whole mount. Fixed brains were embedded in 4% low-melting-point agarose and sectioned (150 μm) along the sagittal axis using a vibratome (1000 Plus, The Vibratome Company, St. Louis, MO, US). These sections were then stained as described in the Supplementary Methods. Cells cultured *in-vitro* were fixed and stained as described(6).

Brain sections and retinas (as whole-mount) were stained as floating samples in 12-well and 96-well plates, respectively. They were blocked overnight at 4 °C in 1% fish-skin gelatin with 0.5% Triton X100 and 5% donkey serum in phosphate-buffered saline (PBS) containing 0.01% thimerosal. The samples were incubated overnight at 4 °C with the primary antibodies diluted in 1% fish-skin gelatin with 0.25% Triton X100 in PBS containing 0.01% thimerosal. Following washing with 0.1% Triton X100 in PBS, the secondary antibodies were added for 4 h at room temperature in 1% fish-skin gelatin with 0.25% Triton X100 in PBS containing 0.01% thimerosal. The incubation with DAPI was in PBS for 4 h, which was followed by several washes in

PBS, post-fixating with 3% paraformaldehyde for 5 min at room temperature, and further washes in PBS. The brain sections were mounted in Vectashield with DAPI, and the coverslips fixed with nail varnish; the retinas were flat-mounted in Prolong gold with DAPI.

Assessment of lesion burden

After staining for immunofluorescence microscopy, brain sections were examined under wide-field fluorescence microscopy (10× and 20×). Lesions have been classified as described in(7) as mulberry (multiple cavernae, group of more than two contiguous cavernae), single caverna (single dilated vessel with maximal diameter accommodating more than 25 red blood cells), or telangiectases, tortuous small vessels with abnormally dilated lumen). The total numbers of lesions were calculated by summing all of the types of lesions.

As the sections were 150-μm thick, a correction was applied to the number of mulberry lesions, which can span two sections. Therefore, the number of mulberry lesions was divided by 1.5. The lesions were counted and classified independently by two observers who were blinded to the treatments.

The maximal diameter of mulberry lesions and single cavernae was used for statistical comparison.

Statistical analysis

Non-parametric Wilcoxon signed-rank tests were used to determine the statistical significance of the lesion burdens after the pharmacological treatments *in-vivo*. Student's two-tailed non-paired t-tests were used to determine the statistical significance in the other *in-vitro* and *in- vivo* analyses. Log-Rank test was used to analyze the Kaplan-Meier survival curves. The significance level was set at $p < 0.05$.

Top/Fop-Flash assay

For the detection of β-catenin-dependent transcription of a reporter target, the Top-Flash plasmid (0.3 $\mu g/cm^2$ cell culture area) was used, which contains seven Tcf/Lef binding sites that control the transcription of firefly luciferase(12) (kindly donated by Dr M.P. Cosma, previously at Telethon Institute for Genetics and Medicine, Naples, Italy, now at Centre for Genomic Research, Barcelona, Spain). This was transfected into the endothelial cells from lung using Lipofectamine 2000, according to the manufacturer instructions (Invitrogen). The pCMV plasmid for constitutive expression of β-gal was co-transfected (0.1 $\mu g/cm^2$), for normalization of luciferase expression over transfection efficiency. As the negative control, a Fop-Flash plasmid containing six mutated (i.e., inactive) Tcf/Lef sites upstream of a minimal promoter and the firefly luciferase gene was used (0.3 $\mu g/cm^2$). This was co-transfected with the β-gal plasmid, for normalization, as above. The Dual-Light Reporter Gene assay system (Applied Biosystems) for the combined detection of firefly luciferase and β-gal was used. The cell extraction and detection of chemiluminescence (Glomax 96 microplate luminometer; Promega) was carried out according to the manufacture instructions.

Active Rap1 pull-down assay

Active Rap1 pull-down assay was performed using the GST-fused Rap1-binding domain of Ral GDS obtained by transforming *E. coli* strain BL21 with a pGEX-2T-RalGDS-RBD expression vector(13). The fusion protein was affinity purified on

Glutathione-Sepharose 4B beads (GE Healthcare) by standard methods. RalGDS-RBD-coupled Glutathione-Sepharose 4B beads (GE Healthcare) were incubated with supernatant to collect GTP-Rap1. Negative control pull-down was with un-coupled Glutathione-Sepharose 4B beads. Briefly, endothelial cells were lysed by addition of 1 volume of cold 2x RIPA lysis buffer to cell suspension. Lysis was performed at 4°C for 10–30 min. Lysates were clarified by centrifugation at maximal speed in an Eppendorf centrifuge for 10 min at 4°C. Five µg of RalGDS-RBD coupled Glutathione-Sepharose 4B beads (GE Healthcare) were added to the supernatant and incubated at 4°C for 30–90 min with slight agitation. Beads were washed four times in 1x RIPA. After the final wash, Laemmli sample buffer was added to the samples. Next, proteins were fractionated by SDS–PAGE and transferred to Protran Nitrocellulose Hybridization Transfer Membrane 0.2 µm pore size (Whatman).

Densitometric analysis was performed using ImageJ imaging software.

Nuclear fractionation

Nuclear fractionation was as described in (14).

References

1. Srinivas S, *et al.* (2001) Cre reporter strains produced by targeted insertion of EYFP and ECFP into the ROSA26 locus. *BMC developmental biology* 1:4.
2. Maddaluno L, *et al.* (2013) EndMT contributes to the onset and progression of cerebral cavernous malformations. *Nature* 498(7455):492-496.
3. Boulday G, *et al.* (2011) Developmental timing of CCM2 loss influences cerebral cavernous malformations in mice. *The Journal of experimental medicine* 208(9):1835-1847.
4. Vleminckx K, Kemler R, & Hecht A (1999) The C-terminal transactivation domain of beta-catenin is necessary and sufficient for signaling by the LEF-1/beta-catenin complex in Xenopus laevis. *Mechanisms of development* 81(1-2):65-74.
5. Liebner S, *et al.* (2008) Wnt/beta-catenin signaling controls development of the blood-brain barrier. *The Journal of cell biology* 183(3):409-417.
6. Lampugnani MG, *et al.* (2010) CCM1 regulates vascular-lumen organization by inducing endothelial polarity. *J Cell Sci* 123(Pt 7):1073-1080.
7. McDonald DA, *et al.* (2012) Fasudil decreases lesion burden in a murine model of cerebral cavernous malformation disease. *Stroke; a journal of cerebral circulation* 43(2):571-574.
8. Wang Y, *et al.* (2010) Ephrin-B2 controls VEGF-induced angiogenesis and lymphangiogenesis. *Nature* 465(7297):483-486.
9. Maretto S, *et al.* (2003) Mapping Wnt/beta-catenin signaling during mouse development and in colorectal tumors. *Proceedings of the National Academy of Sciences of the United States of America* 100(6):3299-3304.
10. Cattelino A, *et al.* (2003) The conditional inactivation of the beta-catenin gene in endothelial cells causes a defective vascular pattern and increased vascular fragility. *The Journal of cell biology* 162(6):1111-1122.
11. Balconi G, Spagnuolo R, & Dejana E (2000) Development of endothelial cell lines from embryonic stem cells: A tool for studying genetically manipulated endothelial cells in vitro. *Arteriosclerosis, thrombosis, and vascular biology* 20(6):1443-1451.
12. Lluis F, Pedone E, Pepe S, & Cosma MP (2008) Periodic activation of Wnt/beta-catenin signaling enhances somatic cell reprogramming mediated by cell fusion. *Cell stem cell* 3(5):493-507.
13. Self AJ, Caron E, Paterson HF, & Hall A (2001) Analysis of R-Ras signalling pathways. (*J Cell Sci* 114(Pt 7):1357-1366..
14. Zhang N, *et al.* (2011) FoxM1 promotes beta-catenin nuclear localization and controls Wnt target-gene expression and glioma tumorigenesis. *Cancer cell* 20(4):427-442.